FEASIBILITY STUDY OF THERMAL AUTOFRETTAGE PROCESS

S. M. Kamal[1*] and U.S. Dixit[2]

[1*]Department of Mechanical Engineering, Indian Institute of Technology Guwahati–781 039
Email: k.seikh@iitg.ac.in
[2]Department of Mechanical Engineering, Indian Institute of Technology Guwahati–781 039
Email: uday@iitg.ac.in

Abstract

Autofrettage is a metal fabrication technique which applies to components subjected to very high pressure such as gun barrels, rocket shells, high pressure piping, high pressure containers etc. The process is carried out either by inducing an ultra-high hydraulic pressure in thick walled cylindrical pressure vessel, called hydraulic autofrettage or by forcing an oversized mandrel through the bore of the cylinder, called swage autofrettage. This causes permanent deformation of the inner layer of the cylinder. The outer layer remains in the elastic state. Thus, compressive residual stresses are generated at the inner layer of the cylinder which reduces the maximum stress involved in the cylinder when it is pressurized in the next loading stage. This work presents a novel method for achieving autofrettage that involves creating temperature gradient in the wall of the cylinder. The proposed process is analyzed theoretically. Preliminary experimental investigation of the process is also carried out. The simulation results and preliminary experiments indicate an encouraging trend for the feasibility of the proposed process.

Keywords: Autofrettage, Thick-walled cylinder, Thermal residual stresses, Elastic-plastic interface

1 Introduction

Autofrettage is a process which is employed to induce the compressive residual stresses in the inner side of the thick walled cylindrical or spherical vessel, thereby increasing the pressure carrying capacity of the vessel. The most commonly used autofrettage process is achieved by inducing ultra-high hydraulic pressure in the vessel. The process was first suggested by Jacob, a French artillery officer, for pre-stressing monobloc gun barrels in 1907 [Malik and Khushnood (2003)]. In hydraulic autofrettage, the process of applying ultra-high hydraulic pressure is complex, slow and expensive and at times dangerous. Later Davidson *et al*. (1962) developed a new approach for achieving autofrettage called swage autofrettage, in which an oversized mandrel is forced through a cylinder to plastically deform the inner wall and some portion beneath it. In swage autofrettage, the preparation of mandrel and swaging assembly makes the process complex. The autofrettage can also be achieved by detonating an explosive charge inside the vessel, which is called explosive autofrettage [Mote *et al.* (1971)].

Residual stresses can also be produced due to thermal gradient in the wall of the cylinder. However, there is hardly any reference in the literature that analyzes this effect. Hussain *et al*. (1980) observed that stress distribution in a partially autofrettaged tube can be analyzed by a simulated thermal loading, such that thermo-elastic stresses produced due to simulated loading will be same as the stress distribution of partially autofrettaged tube. They did not study the thermo-elastic-plastic stresses, which might have indicated the feasibility of thermal autofrettage. Thus, there is no experimental or theoretical study on thermal autofrettage in open literature. Thermal autofrettage is a potential process offering many advantages compared to hydraulic and swage autofrettage, such as absence of high pressure and moving parts. This paper analyzes thermal autofrettage for exploring the feasibility of its industrial exploitation.

2 Proposed thermal autofrettage process

The proposed method of autofrettage is based on the stress field generated due to the temperature gradient developed between outer and inner wall of the cylinder or hollow disk. The schematic diagram of the method is shown in Fig. 1. In order to understand the mechanics of thermal autofrettage, plane stress assumption will be employed in Section 3. Plane stress assumption is appropriate for thin circular hollow disk. It may provide reasonable solution for short cylinders as well.

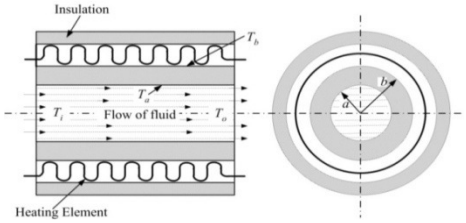

Fig 1 A schematic diagram of thermal autofrettage process

An open ended thin hollow disk or short cylinder is considered having inner radius a and outer radius b. The disk is heated externally and flow of cold fluid is continuously regulated such that outer wall of the disk is subjected to a temperature T_b and inner wall is subjected to a temperature T_a. At a sufficiently large temperature difference between the outer and inner walls of the disk, the inner portion of the disk always yields first and it becomes plastic up to some intermediate radius, whilst the outer portion of the disk remains in the elastic state if the temperature difference is not large enough to cause the yielding of outer wall of the disk. The temperature difference required for initial yielding is identified by using Tresca's yield criterion and is explained in detail in Section 3.1. When the temperature difference is increased beyond certain limit, the outer wall of the disk begins to yield and the plastic deformation of both the inner and outer portion of the disk undergoes simultaneously leaving the intermediate portion of the disk in the elastic state. When the entire cylinder is cooled to room temperature, compressive residual stresses are produced in the cylinder.

The proposed method is very simple and easy to handle compared to the existing methods of autofrettage. In the following subsections, stress as well as thermal analysis of the process is carried out.

3 Thermo Elasto-plastic analyses in the disk

Consider an open ended thin circular disk (σ_z=0) of homogeneous material. The inner radius of the disk is a and the outer radius is b. The disk is subjected to Dirichlet temperature boundary conditions. The outer wall of the disk is maintained at temperature T_b and the inner wall is maintained at temperature T_a such that T_b>T_a. The steady-state temperature distribution in the disk is given by [Chakrabarty (2006)]

$$T = T_b + (T_a - T_b)\frac{\ln\left(\frac{b}{r}\right)}{\ln\left(\frac{b}{a}\right)}. \tag{1}$$

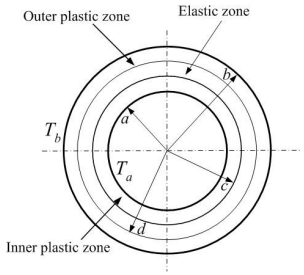

Figure 2 The inner plastic, intermediate elastic and outer plastic zones in the hollow disk

In a generalized situation, there are three zones of deformation in the wall of the disk– inner plastic zone, intermediate elastic zone and outer plastic zone. When the temperature difference is small, the entire thickness is elastic. After certain threshold temperature, first stage of plastic deformation begins creating an inner plastic and outer elastic zone. When the temperature difference crosses the second threshold, second stage of plastic deformation commences and the most general case of inner plastic, intermediate elastic and outer plastic is obtained. The most general case is shown in Fig. 2. In this work, it is assumed that the material yields as per Tresca criterion.

3.1 Elastic solution

With zero temperature as a reference and using generalized Hook's law, the radial and hoop strains in the elastic zone at temperature T are given as [Noda *et al.* (2003)]

$$\varepsilon_r = \frac{1}{E}(\sigma_r - \nu\sigma_\theta) + \alpha T, \tag{2}$$

$$\varepsilon_\theta = \frac{1}{E}(\sigma_\theta - \nu\sigma_r) + \alpha T, \tag{3}$$

where σ_r is the radial stress, σ_θ is the hoop stress, ν is the Poisson's ratio, E is the Young's modulus of elasticity and α is the coefficient of thermal expansion. For radial displacement u as a function of r, the radial and hoop strains are given by [Chakrabarty (2006)]

$$\varepsilon_r = \frac{\mathrm{d}u}{\mathrm{d}r}, \quad \varepsilon_\theta = \frac{u}{r}. \tag{4}$$

Hence, the strain compatibility in cylindrical polar co-ordinate system can be written as

$$\varepsilon_r - \varepsilon_\theta = r\frac{\mathrm{d}\varepsilon_\theta}{\mathrm{d}r}. \tag{5}$$

The equilibrium equation is given as [Chakrabarty (2006)]

$$\sigma_\theta - \sigma_r = r\frac{\mathrm{d}\sigma_r}{\mathrm{d}r}. \tag{6}$$

Using Eqs. (2, 3) in Eq. (5) and solving it along with Eq. (6) with the boundary conditions σ_r=0 at r=a & σ_r=0 at r=b, the solution for elastic thermal stresses σ_r and σ_θ is given by [Noda *et al.* (2003)]:

$$\sigma_r = \frac{E\alpha}{2}(T_b - T_a)\left\{-\frac{\ln\left(\frac{r}{a}\right)}{\ln\left(\frac{b}{a}\right)} + \left(1 - \frac{a^2}{r^2}\right)\frac{b^2}{b^2 - a^2}\right\}, \tag{7}$$

$$\sigma_\theta = \frac{E\alpha}{2}(T_b - T_a)\left\{-\frac{1 + \ln\left(\frac{r}{a}\right)}{\ln\left(\frac{b}{a}\right)} + \left(1 + \frac{a^2}{r^2}\right)\frac{b^2}{b^2 - a^2}\right\}. \tag{8}$$

A typical distribution of these stresses is shown in Fig. 3 for an aluminum disk having a=10 mm, b=20 mm, E=69

GPa, (T_b-T_a)=40°C and α=22.2×10^{-6}/°C. It is observed that always there is a possibility of yielding of the disk at the inner wall first compared to the outer wall when the temperature difference is increased. The distribution of thermal stresses in an open ended hollow disk is such that at and around inner radius, $\sigma_\theta>\sigma_r>\sigma_z$. Hence, the temperature difference required for the initiation of the yielding at the inner radius ($r=a$) is estimated by using Tresca's yield criterion, $\sigma_\theta-\sigma_z=k_1\sigma_Y$, where σ_Y is the yield stress and k_1 is a sign factor that can be +1 or −1 depending on whether $T_b>T_a$ or $T_b<T_a$. Similarly, the temperature difference required for initial yielding at the outer radius ($r=b$) can be estimated.

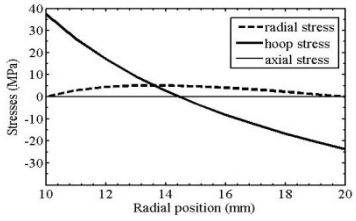

Fig 3 Thermal stresses in a hollow disk

3.2 Analyses of the zones during first stage of plastic deformation

During first stage of plastic deformation, the inner wall of the disk becomes plastic up to a radius c. Thus, the disk is composed of an inner plastic zone $a<r<c$, surrounded by an outer elastic zone $c<r<b$. The radius c is known as the radius of elastic-plastic interface.

3.2.1 Elastic zone: $c<r<b$

For the outer elastic zone the thermal stresses are obtained, by using boundary conditions, $(\sigma_\theta)_{r=c}= k_1\sigma_Y$ and $(\sigma_r)_{r=b}$ = 0 and solving equilibrium equation (Eq. 6), compatibility condition (Eq. 5) and stress-strain equations (Eqs. 2 and 3). These are given as

$$\sigma_r=\frac{E\alpha(T_b-T_a)}{2\ln\left(\frac{b}{a}\right)}\left[\ln\left(\frac{b}{r}\right)+\left(\frac{c^2}{b^2+c^2}\right)\left(1-\frac{b^2}{r^2}\right)\left\{1-\ln\left(\frac{b}{c}\right)\right\}\right] + \frac{c^2k_1\sigma_Y}{b^2+c^2}\left(1-\frac{b^2}{r^2}\right), \quad (9)$$

$$\sigma_\theta=\frac{E\alpha(T_b-T_a)}{2\ln\left(\frac{b}{a}\right)}\left[\ln\left(\frac{b}{r}\right)-1+\left(\frac{c^2}{b^2+c^2}\right)\left(1+\frac{b^2}{r^2}\right)\left\{1-\ln\left(\frac{b}{c}\right)\right\}\right] + \frac{c^2k_1\sigma_Y}{b^2+c^2}\left(1+\frac{b^2}{r^2}\right). \quad (10)$$

The displacement component in the outer elastic zone is obtained using Eqs. (9) and (10) in Eq. (3) and second relation of Eq. (4) as

$$u=\frac{\alpha(T_b-T_a)}{2\ln\left(\frac{b}{a}\right)}\left[\begin{aligned}&(1-\nu)r\ln\left(\frac{b}{r}\right)-r+(1-\nu)r\left(\frac{c^2}{b^2+c^2}\right)\left\{1-\ln\left(\frac{b}{c}\right)\right\}\\&+\left(\frac{c^2}{b^2+c^2}\right)\left\{1-\ln\left(\frac{b}{c}\right)\right\}\left\{(1-\nu)r+(1+\nu)\frac{b^2}{r}\right\}\end{aligned}\right] + \frac{c^2k_1\sigma_Y}{E\left(b^2+c^2\right)}\left\{(1-\nu)r+(1+\nu)\frac{b^2}{r}\right\}+r\alpha T. \quad (11)$$

3.2.2 Plastic zone: $a<r<c$

For the plastic zone ($a<r<c$), considering the material strain hardening, Tresca's yield criterion for an open ended disk provides

$$\sigma_\theta=k_1\sigma_{eq}, \quad (12)$$

where σ_{eq} ($>\sigma_Y$) is the equivalent stress in uniaxial tension or compression. It is assumed that the hardening of the disk material follows the Ludwik's hardening law [Dixit & Dixit (2008)] given by

$$\sigma_{eq}=\sigma_Y+K\left(\varepsilon_{eq}^p\right)^n, \quad (13)$$

where K is the hardening coefficient and n is the strain hardening exponent. Using Eq. (6) and Eq. (12) and the boundary condition σ_r at $r=c$ from elastic zone (Eq. 9), the solution for radial thermal stress in the plastic zone is obtained as

$$\sigma_r=\left(\frac{c}{r}\right)\frac{E\alpha(T_b-T_a)}{2\ln\left(\frac{b}{a}\right)}\left[\ln\left(\frac{b}{c}\right)+\left(\frac{c^2}{b^2+c^2}\right)\left(1-\frac{b^2}{c^2}\right)\left\{1-\ln\left(\frac{b}{c}\right)\right\}\right] + k_1\sigma_Y\left\{1-\left(\frac{2b^2}{b^2+c^2}\right)\left(\frac{c}{r}\right)\right\}-k_1\frac{K}{r}\int_r^c\left(\varepsilon_{eq}^p\right)^n\mathrm{d}r\,. \quad (14)$$

The thermal hoop stress in the plastic zone is given by Eq. (12).

In the plastic zone, the total strain is composed of elastic and plastic strains

$$\varepsilon_r=\frac{\mathrm{d}u}{\mathrm{d}r}=\varepsilon_r^e+\varepsilon_r^p,\quad \varepsilon_\theta=\frac{u}{r}=\varepsilon_\theta^e+\varepsilon_\theta^p. \quad (15)$$

The elastic components and are given by Eqs. (2) and (3). In view of Tresca's associated flow rule [Chakrabarty (2006)], $\mathrm{d}\varepsilon_r^p=0$, $\mathrm{d}\varepsilon_\theta^p=-\mathrm{d}\varepsilon_z^p$. Hence, ε_r is entirely elastic. Substituting Eq. (15) in Eqs. (2) and (3) and then using Eq. (6), the following differential equation is obtained:

$$\frac{\mathrm{d}}{\mathrm{d}r}\left\{\frac{1}{r}\frac{\mathrm{d}}{\mathrm{d}r}(ur)\right\}=\nu\frac{\mathrm{d}\varepsilon_\theta^p}{\mathrm{d}r}+\alpha(1+\nu)\frac{\mathrm{d}T}{\mathrm{d}r}-\left(\frac{1-\nu}{r}\right)\varepsilon_\theta^p. \quad (16)$$

Eq. (16) is solved along with the total strain compatibility condition (Eq. 5) and using the continuity of σ_r and u at $r=c$ (Eqs. 9 and 11), the solution for total hoop strain is obtained as

$$\varepsilon_\theta^p=\frac{u}{r}=\frac{\alpha(T_b-T_a)}{2\ln\left(\frac{b}{a}\right)}\left[\left\{\frac{2c^2b^2}{r^2\left(b^2+c^2\right)}\right\}\left\{1-\ln\left(\frac{b}{c}\right)\right\}+2\ln\left(\frac{r}{a}\right)-1\right] + \frac{2}{E}\frac{k_1c^2b^2\sigma_Y}{r^2\left(b^2+c^2\right)}+\frac{1-\nu}{E}\sigma_r+\alpha T_a-\frac{1}{r^2}\int_r^c r\varepsilon_\theta^p\mathrm{d}r. \quad (17)$$

The plastic hoop strain field is obtained by subtracting the elastic part from the total strain component. This is given by

$$\varepsilon_\theta^p = \frac{\alpha(T_b - T_a)}{2\ln\left(\frac{b}{a}\right)}\left[\left\{\frac{2c^2b^2}{r^2\left(b^2+c^2\right)}\right\}\left\{1-\ln\left(\frac{b}{c}\right)\right\}-1+\frac{c}{r}\ln\left(\frac{b}{c}\right)+\left\{\frac{c^3}{r\left(b^2+c^2\right)}\right\}\left(1-\frac{b^2}{c^2}\right)\left\{1-\ln\left(\frac{b}{c}\right)\right\}\right]+\frac{2}{E}\frac{k_1c^2b^2\sigma_Y}{r^2\left(b^2+c^2\right)} \quad (18)$$

$$+\frac{k_1c^3\sigma_Y}{Er\left(b^2+c^2\right)}\left(1-\frac{b^2}{c^2}\right)-\frac{k_1\sigma_Y}{E}\left(\frac{c}{r}\right)-k_1\frac{K}{Er}\int_r^c\left(\varepsilon_{eq}^p\right)^n\mathrm{d}r-\frac{1}{r^2}\int_r^c r\varepsilon_\theta^p\mathrm{d}r-k_1\frac{K}{E}\left(\varepsilon_{eq}^p\right)^n.$$

The equivalent plastic strain field for the present case is given by

$$\varepsilon_{eq}^p = \frac{2}{\sqrt{3}}\varepsilon_\theta^p. \quad (19)$$

3.3 Analyses of the zones during second stage of plastic deformation

When the temperature difference exceeds the threshold value, the second stage of plastic deformation starts in the disk. This results an inner plastic zone $a<r<c$, an outer plastic zone $d<r<b$ and an intermediate elastic zone $c<r<d$ in the disk. The radii, c and d are the radii of elastic-plastic interfaces.

3.3.1 Elastic zone: $c<r<d$

Following the same procedure as in Section 3.2.1 and using the boundary conditions $(\sigma_\theta)_{r=c} = k_1\sigma_Y$ and $(\sigma_\theta-\sigma_r)_{r=d} = -k_1\sigma_Y$, the thermal stresses for the intermediate elastic zone ($c<r<d$) is obtained as

$$\sigma_r = \frac{E\alpha(T_b-T_a)}{2\ln\left(\frac{b}{a}\right)}\left\{1+\ln\left(\frac{c}{r}\right)-\frac{d^2}{2c^2}-\frac{d^2}{2r^2}\right\}+k_1\sigma_Y\left(1+\frac{d^2}{2c^2}+\frac{d^2}{2r^2}\right), \quad (20)$$

$$\sigma_\theta = \frac{E\alpha(T_b-T_a)}{2\ln\left(\frac{b}{a}\right)}\left\{\ln\left(\frac{c}{r}\right)-\frac{d^2}{2c^2}+\frac{d^2}{2r^2}\right\}+k_1\sigma_Y\left(1+\frac{d^2}{2c^2}-\frac{d^2}{2r^2}\right). \quad (21)$$

The displacement component for this elastic zone is obtained using Eqs. (20) and (21) in Eq. (3) and second relation of Eq. (4) as

$$u = \frac{\alpha(T_b-T_a)}{2\ln\left(\frac{b}{a}\right)}\left\{(1+\nu)\frac{d^2}{2r}-(1-\nu)\frac{d^2r}{2c^2}+(1-\nu)r\ln\left(\frac{c}{r}\right)-\nu r\right\} \quad (22)$$

$$+\frac{k_1\sigma_Y}{E}\left\{(1-\nu)r+(1-\nu)\frac{d^2r}{2c^2}-(1+\nu)\frac{d^2}{2r}\right\}+\alpha r\left\{T_a+(T_b-T_a)\frac{\ln\left(\frac{r}{a}\right)}{\ln\left(\frac{b}{a}\right)}\right\}.$$

3.3.2 Inner plastic zone: $a<r<c$

For the inner plastic zone ($a<r<c$), following the same procedure as in the Section 3.2.2, the solution for radial thermal stress and plastic hoop strain is obtained as

$$\sigma_r = \left(\frac{c}{r}\right)\frac{E\alpha(T_b-T_a)}{2\ln\left(\frac{b}{a}\right)}\left(1-\frac{d^2}{c^2}\right)+k_1\sigma_Y\left(1+\frac{d^2}{cr}\right)-k_1\frac{K}{r}\int_r^c\left(\varepsilon_{eq}^p\right)^n\mathrm{d}r, \quad (23)$$

$$\varepsilon_\theta^p = \frac{\alpha(T_b-T_a)}{2\ln\left(\frac{b}{a}\right)}\left\{\frac{d^2}{r^2}-1+\left(\frac{c}{r}\right)\left(1-\frac{d^2}{c^2}\right)\right\}+\frac{k_1\sigma_Y}{E}\left(\frac{d^2}{cr}-\frac{d^2}{r^2}\right) \quad (24)$$

$$-\frac{1}{r^2}\int_r^c r\varepsilon_\theta^p\mathrm{d}r-k_1\left(\frac{2}{\sqrt{3}}\right)^n\frac{K}{rE}\int_r^c\left(\varepsilon_\theta^p\right)^n\mathrm{d}r-k_1\left(\frac{2}{\sqrt{3}}\right)^n\frac{K}{E}\left(\varepsilon_\theta^p\right)^n.$$

The thermal hoop stress is given by Eq. (12).

3.3.3 Outer plastic zone: $d<r<b$

For the outer plastic zone ($d<r<b$), considering the effect of strain hardening of the cylinder material Tresca's yield criterion is given by

$$\sigma_\theta - \sigma_r = -k_1\sigma_{eq}. \quad (25)$$

Using Eqs. (6), (13) & (25) and the boundary condition σ_r at $r = d$ from elastic zone (Eq. 20), the solution for thermal stresses in the outer plastic zone is obtained as

$$\sigma_r = \frac{E\alpha(T_b-T_a)}{2\ln\left(\frac{b}{a}\right)}\left\{\frac{1}{2}+\ln\left(\frac{c}{d}\right)-\frac{d^2}{2c^2}\right\} \quad (26)$$

$$+k_1\sigma_Y\left\{\frac{3}{2}+\frac{d^2}{2c^2}-\ln\left(\frac{r}{d}\right)\right\}+k_1K\int_r^d\frac{1}{r}\left(\varepsilon_{eq}^p\right)^n\mathrm{d}r,$$

$$\sigma_\theta = \frac{E\alpha(T_b-T_a)}{2\ln\left(\frac{b}{a}\right)}\left\{\frac{1}{2}+\ln\left(\frac{c}{d}\right)-\frac{d^2}{2c^2}\right\}+k_1\sigma_Y\left\{\frac{1}{2}+\frac{d^2}{2c^2}-\ln\left(\frac{r}{d}\right)\right\} \quad (27)$$

$$+k_1K\int_r^d\frac{1}{r}\left(\varepsilon_{eq}^p\right)^n\mathrm{d}r-k_1K\left(\varepsilon_{eq}^p\right)^n.$$

In the outer plastic zone, Tresca's associated flow rule provides, $\mathrm{d}\varepsilon_z^p = 0$, $\mathrm{d}\varepsilon_\theta^p = -\mathrm{d}\varepsilon_r^p$. Hence, due to plastic incompressibility $\varepsilon_r^p + \varepsilon_\theta^p = 0$. Thus,

$$\varepsilon_r + \varepsilon_\theta = \varepsilon_r^e + \varepsilon_r^p + \varepsilon_\theta^e + \varepsilon_\theta^p = \varepsilon_r^e + \varepsilon_\theta^e. \quad (28)$$

Using Eq. (4) & (6) and inserting Eqs. (2) and (3) in Eq. (34), the following differential equation is obtained:

$$\frac{\mathrm{d}}{\mathrm{d}r}(ur) = 2\alpha Tr+\frac{1}{E}(1-\nu)\frac{\mathrm{d}}{\mathrm{d}r}\left(r^2\sigma_r\right). \quad (29)$$

Eq. (29) is solved using the continuity of σ_r and u at $r=c$ (Eqs. 20 and 22), to obtain the total hoop strain component as

$$\frac{u}{r} = \alpha T_a+\frac{\alpha(T_b-T_a)}{2\ln\left(\frac{b}{a}\right)}\left\{2\ln\left(\frac{r}{a}\right)-1+\frac{d^2}{r^2}\right\}+\frac{1}{E}(1-\nu)\sigma_r-\frac{k_1\sigma_Y}{E}\frac{d^2}{r^2}. \quad (30)$$

The plastic part of the hoop strain is obtained by subtracting the elastic part from the total hoop strain component. This is given by

$$\varepsilon_\theta^p = \frac{\alpha(T_b-T_a)}{2\ln\left(\frac{b}{a}\right)}\left(\frac{d^2}{r^2}-1\right)+\frac{k_1\sigma_Y}{E}\left(1-\frac{d^2}{r^2}\right)+\frac{k_1K}{E}\left(\varepsilon_{eq}^p\right)^n. \quad (31)$$

The equivalent plastic strain is given by Eq. (19).

3.4 Determination of thermal residual stresses

When the temperature difference induced in the hollow disk due to heating vanishes after cooling, residual

thermal stresses are generated in the disk. It is assumed that the unloading process is completely elastic and linear devoid of Bauschinger effect. Thus, the thermal residual radial and hoop stresses for each zone are evaluated by subtracting Eqs. (7) and (8) from the respective equations for radial and hoop stresses in the zone.

4. Solution methodology

There is a need to use numerical methods for finding out elastic-plastic interfaces c and d and plastic strains. The following solution methodology is employed:

Step 1: For the case when only inner portion is plastic during the application of thermal gradient, the initial estimate for radius of elastic-plastic interface, c, is obtained by making σ_r=0 at r=a in Eq. (14) for non-hardening case (K=0) and solving it using FZERO function (based on bisection method) in MATLAB. However, when both inner and outer portion are plastic, the initial estimates for c & d, are obtained by making σ_r=0 at r=a, in Eq. (23) and σ_r=0 at r=d, in Eq. (26) for non-hardening case (K=0) and solving them for c & d using FSOLVE function (the least square method of solving simultaneous nonlinear equations) in MATLAB. The initial guess value of is taken as zero.

Step 2: The updated plastic strain field at different radial positions is found out from Eq. (18) when only inner zone is plastic and from Eqs. (24) and (31) when inner as well as outer zones are plastic. For the fixed c, in Eq. (18) and for the fixed values of c & d, in Eqs. (24) and (31), values of ε_θ^p is updated further and this process is repeated till convergence in is achieved. This basically amounts to solving for using fixed point iteration method [Gerald & Wheatley (1994)]. The integrations involved in Eqs. (18, 24 and 31) are evaluated numerically using trapezoidal rule.

Step 3: Now using the values of ε_θ^p at different radial positions in the corresponding plastic zones the integral terms in Eqs. (14, 23 and 26) are evaluated and the expressions are solved for new estimated values of c or c & d by making radial stresses zero at r=a or at r=a & r=d respectively. If the new estimated values of c or c & d are same as the previous estimated values, go to step 4. Otherwise go to Step 2 and repeat the process till the convergence for c or c & d is achieved.

Step 4: Using the latest updated values of ε_θ^p , c or c & d, the radial and hoop stresses in the plastic zones for the corresponding cases are calculated from Eqs. (12), (14), (23), (26) and (27).

5. Numerical simulation

The proposed autofrettage process is simulated numerically for mild steel disk using the equations developed in Section 3. The corresponding equations are solved following the methodology discussed in Section 4. The simulated results are discussed in the following.

A mild steel disk with inner radius, a=10 mm and outer radius, b = 30 mm is simulated, when it undergoes autofrettage process due to a temperature difference between the outer and inner surface. Material properties considered for steel are as follows: Young's modulus of elasticity, E = 200 GPa, yield stress, σ_Y =324 MPa, coefficient of thermal expansion, α = 13×10^{-6}/ºC. The temperature difference required for initial yielding at the inner wall of the disk for this case is 186 ºC. The temperature difference required to cause the initial yielding of the outer wall of the disk is obtained as 377.5 ºC, which is quite large. The large temperature difference may greatly change the material properties. Therefore, it is not advisable to induce such a large temperature difference to cause the yielding of the outer wall. Hence, the disk is simulated for a temperature difference of 270 ºC for achieving autofrettage which will cause the plastic deformation of inner portion only. The radius of elastic-plastic interface, c is obtained as 11.709 mm. The hardening coefficient K and strain hardening exponent n for the disk are taken as 226.98 MPa and 0.43. The stresses generated in the disk as a result of autofrettage are shown as a function of radial position.

The elastic-plastic thermal stress pattern in the disk is shown in Fig. 4(a). It is observed that the magnitude of radial stresses is quite small compared to hoop stresses. The radial stresses are always tensile, whilst the hoop stresses change from tensile to compressive along the positive radial direction. This trend gets reversed when the temperature difference is removed. This is shown in Fig. 4(b). It is observed that a significant amount of compressive residual hoop stresses are generated in and around the inner radius of the cylinder and hence it reduces the magnitude of resultant stress when it is subjected to internal working pressure. The magnitudes of tensile residual stresses generated at the outer region of the cylinder are very small.

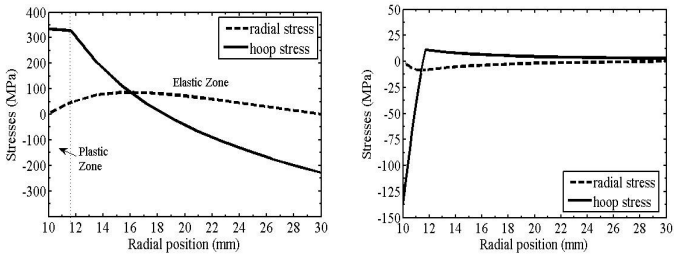

(a) (b)

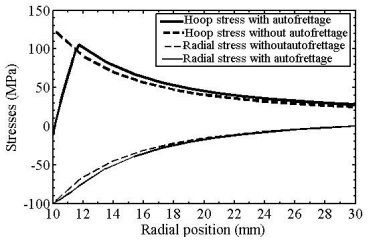

(c)

Fig 4 (a) Elastic-plastic stress, (b) Residual stress and (c) Overall stresses in steel disk

The autofrettaged steel disk is now subjected to an internal working pressure of 100 MPa and the resultant stress pattern is shown in Fig. 4(c). The corresponding stresses without autofrettage are also shown using well-known Lame's equations.

$$\sigma_r = \frac{p_i a^2}{b^2 - a^2}\left(1 - \frac{b^2}{r^2}\right), \quad \sigma_\theta = \frac{p_i a^2}{b^2 - a^2}\left(1 + \frac{b^2}{r^2}\right), \tag{32}$$

where p_i is the internal working pressure. In case of the autofrettaged disk, the magnitude of the maximum equivalent Tresca stress is found to be 18.82% less than that in case of the disk without autofrettage during pressurization. The maximum equivalent Tresca stress exists at the radius of elastic-plastic interface for the autofrettaged case. Therefore, yielding of the disk during pressurization will first take place at the elastic-plastic interface. The maximum pressure carrying capacity of the autofrettaged disk in this case is 186 MPa. The non-autofrettaged disk can withstand a maximum pressure of 144 MPa only.

6 Preliminary experiments

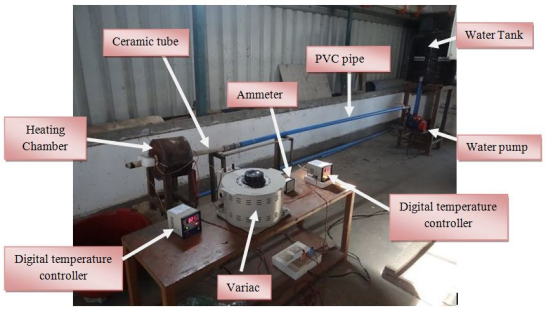

Fig 5 The experimental setup

In order to assess the feasibility of thermal autofrettage, an experimental setup has been developed at IIT Guwahati and is shown in Fig. 5. For creating temperature gradient in the cylinder, the cylinder is heated in the heating chamber by means of electrical heating element and the inner surface is made cooler by regulating continuous flow of cold water. In the present experiment, the length of the cylinder considered is not large enough and no significant temperature variation of cold water flow from inlet to outlet is observed. Thus there will be uniform yielding along the length of the cylinder. For the experiment, a mild steel disk (short cylinder!) of inner radius 5 mm and outer radius 20 mm is considered. The length of the cylinder is 50 mm. A temperature difference of 268 ºC was generated between the outer and inner wall of the disk, which is sufficient for achieving thermal autofrettage. After that the cylinder was allowed to cool to the room temperature. The micro-hardness tests were conducted on the outer and inner surface of the autofrettaged disk using Vickers micro-hardness tester at a load of 500 gf. The micro-hardness test of the non-autofrettaged disk material was also carried out. The average micro-hardness of the non-autofrettaged disk was 170.64 HV with standard deviation 5.25 HV. The hardness of the outer surface of the autofrettaged disk was 157.28 HV with standard deviation 7.32, whereas the hardness of the inner surface was 219.52 HV with standard deviation 12.84. It is envisaged that tensile residual stresses on the outer surface cause a decrease in the micro-hardness. Similarly, the compressive residual stresses on the inner surface cause an increase in the micro-hardness. Thus, it appears that the partial thermal autofrettage has been achieved.

7. Conclusion

In the present work a novel autofrettage process by inducing temperature difference in the hollow circular disk (or short cylinder) is proposed. The process is analyzed theoretically considering the strain hardening of the disk during plastic deformation. Simulations are carried out for thermal autofrettage of a mild steel disk. The overall simulation results show trends similar to those observed by other researchers in case of hydraulic autofrettage. Some preliminary experiments are also carried out to see the feasibility of the proposed process. The results of the preliminary experiment are encouraging. Compared to hydraulic and swage autofrettage, the achievable level of autofrettage is limited by the maximum allowable temperature at the outer surface of the disk. However, the simplicity of the process has potential to make it a competitive process.

References

Chakrabarty, J. (2006), Theory of Plasticity, 3rd edition. Butterworth-Heinemann, Burlington.

Davidson, T.E., Barton, C.S., Reiner A.N. and Kendall, D.P. (1962), New approach to the autofrettage of high-

strength cylinders, *Experimental Mechanics*, Vol. 2, pp. 33–40.

Dixit, P. M. and Dixit, U. S. (2008), Modeling of Metal Forming and Machining Processes: By Finite Element and Soft Computing Methods. Springer, London.

Gerald, C. F. and Wheatley, P. O. (1994), Applied Numerical Analysis, fifth edition, Addison-Wesley, England.

Hussain, M. A., Pu, S. L., Vasilakis, J. D. and O'Hara, P. (1980), Simulation of partial autofrettage by thermal loads, *ASME Journal of Pressure Vessel Technology*, Vol. 102, pp. 314–318.

Kaplan, M. A. (1971), Explosive autofrettage of cannon barrels, AMMRC CR 70-25, Army Materials and Mechanics Research Center, Watertown, Massachusetts.

Malik, M. A. and Khushnood, S. (2003), A review of swage-autofrettage process, *Proceedings of 11th International Conference on Nuclear Engineering*, Tokyo, April, pp. 20–23.

Mote, J. D., Ching, L. K. W., Knight, R. E., Fay R. J. and Noda, N., Hetnarski, R. B. and Tanigawa, Y. (2003), Thermal Stresses, 2nd edition. Taylor and Francis, New York.